Journal of Multidisciplinary Engineering Science Studies (JMESS)
ISSN: 2458-925X
Vol. 7 Issue 11, November - 2021

Two Self-Oscillatory Regimes Of Supersonic Flows Near The Pair Cylinder – Open Channel

Vladimir I. Pinchukov
Federal Investig. Centre of Inform. & Comput. Technol.,
Siberian Branch of RAS, Novosibirsk, Russia
E-mail-addresses: pinchvi@ict.nsc.ru, pinch_v_i@mail.ru

***Abstract*—Supersonic flows near a cylinder, placed near the end of channel, are studied. Channels of rotation with the interval of cross-sectional area decreasing are considered. Two-dimensional Euler equations are solved by two methods, namely, by the explicit two step Godunov type method and by the implicit Runge-Kutta method. Artificial viscosity of Smagorinsky type is applied in both methods. Self-oscillatory regimes are studied at free-stream Mach numbers of 3.5 to 4.5. Two types of unsteady regimes are observed.**

Keywords—self-oscillations, Euler equations, numerical studies, channels;

1. Introduction

This paper is devoted to continuation of CFD studies of new unsteady flows, carried out in [1-7]. Namely, new family of self-oscillatory flows near the pair cylinder - open channel was found in [6], where the interval of free stream Mach numbers $3 \le M_\infty \le 4.5$ was considered. Hypersonic flows with free stream Mach numbers $5 \le M_\infty \le 7.5$ are studied in [7]. It is found in [6,7], that unsteady regimes exist, only if intersection points of available in these flows two shock waves are not too far from the tube edge. Two types of self-oscillatory flows are observed in [7]. If contact discontinuity, issued from the intersection point, is directed always above the tube edge, flows of the first type take place. If this contact discontinuity is directed inside or outside a tube alternately, second type of unsteady flows takes place. Present paper is devoted to a search of these regimes in the interval $3.5 \le M_\infty \le 4.5$.

It seems, that flows of the first type of this family have the oscillation mechanism, similar to this mechanism of flows around spiked bodies [1,8-10].

2. CFD design approach

Numerical calculations deal with dimensionless variables. These variables are defined as relations of initial variables and next free stream parameters or the body size: p_∞ - for pressure, ρ_∞ - for density, $\sqrt{p_\infty/\rho_\infty}$ - for a velocity, r_{tub}=y(*C*)-y(*H*) (the maximum inner channel radius, see fig. 1) – for space variables, $r_{tub}/\sqrt{p_\infty/\rho_\infty}$ - for time.

2.1. Boundary conditions.

Fig. 1 represents schematically a numerical domain and a mesh near a cylindrical body, placed in an open channel. All variables are prescribed at the inflow boundary (*HA*). Parameters of the uniform stream are set at this boundary, namely, Mach number $M=M_\infty$, density $\rho=1$, pressure $p=p_\infty=1$ (in dimensionless form), the radial velocity v=0. The normal velocity is equal to zero and other variables are extrapolated at solid surfaces (*CB,CD,FE,FG*). The radial velocity v=0 at the symmetry axis *HG*, other variables are extrapolated. Extrapolation conditions are used at the tube exit *DE* and at the *AB* boundary.

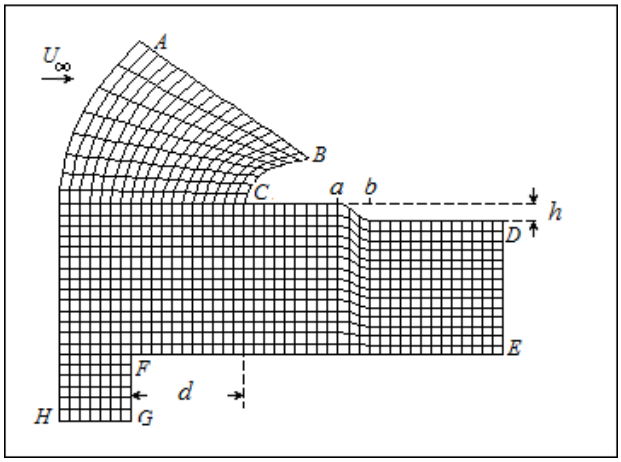

Fig. 1. *Schematic representation of a numerical domain and of a mesh.*

The channel form at the [*a,b*] interval of cross-sectional area decreasing is defined by the formulae

$$Y(x)=R_{tub}\text{-}16h(x\text{-}a)^2(x\text{-}2b+a)^2/(b\text{-}a)^4. \qquad (1)$$

2.2. Numerical methods.

Every flow is calculated here by two methods: by the second order two step version of the Godunov conservative method [11] and by the implicit conservative Runge-Kutta method [12], which is third order of approximation initially, but this order is reduced to the second one as a result of usage of Smagorinsky viscosity. Comparing of these two methods data allows to evaluate accuracy of numerical results. Approximate linear solution of the Riman problem is applied in the Godunov method. Algorithms of slopes limitation of left and right extrapolation curves are used to damp false oscillations near discontinuities. Review of such algorithms of damping false oscillations is presented in [13].

Both methods are modified to provide possibility of solution calculations in complicated domains. Namely, special versions of codes are developed for the case when functions $x=x(\xi,\eta)$, $y=y(\xi,\eta)$ perform mapping of the unit square with excisions $\{0\le\xi\le\xi_0,\ 0\le\eta\le\eta_0\}$, $\{\xi_1\le\xi\le1,\ 0\le\eta\le\eta_1\}$ to a curvilinear quadrangle with curvilinear quadrangular excisions (see fig. 1). These codes allow carrying out calculations without dividing complicated domains into subdomains.

2.3 Adaptive version of Smagorinsky viscosity.

Navier-Stokes viscous terms are included to Euler equations and the artificial viscosity of Smagorinsky type [14] is used for additional damping of false oscillations. To ensure absence of false oscillations, the adaptive version of Smagorinsky viscosity is applied:

$$\mu=\rho|S|\Delta^2[wC_1^2+(1\text{-}w)C_2^2],\ |S|=(2S_{ik}S_{ik})^{1/2}, \qquad (2)$$

$$\Delta=\Delta\xi\,\Delta\eta\,(x_\zeta y_\eta - y_\zeta x_\eta)/$$

$$(\max(\Delta\xi^2(x_\zeta^2+y_\zeta^2),\Delta\eta^2(x_\eta^2+y_\eta^2)))^{1/2},$$

$$S_{ik}=\partial u_i/\partial x_k+\partial u_k/\partial x_i)/2,$$

where functions $x=x(\xi,\eta)$, $y=y(\xi,\eta)$ perform coordinate transformation, $\Delta\xi=1/N_\zeta$, $\Delta\eta=1/N_\eta$, N_ζ, N_η - numbers of intervals of the quadrangular mesh in a unit square, $1\ge C_1\ge C_2\ge0$ – two constants, defining distribution of turbulent viscosity in the flow, w – weight function.

Weight function *w* should have most values, closed to unity, in vicinities of shift layers and should have least, but positive, values beyond these vicinities. Different versions of this function were tried. Preferable results are achieved, if this function has variables |S|, |rot U|. To illustrate the relation of this parameters let consider the ideal shift layer {u(x,y)=u°(y), v(x,y)=0, 0 ≤y≤1, -∞≤x≤∞}. It is easy to receive, that the equality |S|=|rot U| takes place since only single derivative $\partial u/\partial y$ distinguishes from zero. Of course, this equality is not true for real shift layers. Nevertheless the relation |(|S|-|rot U|)| «(|S|+|rot U|) takes place for large Reynolds numbers. So next simple formulae satisfies to requirements written above:

$$w=1/[1+C_o(|\text{rot U}|^2/|S|^2\text{-}1)^2], \qquad (3)$$

where C_o should be chosen in trial computations.

It should be noted, that RANS have parabolic type, if turbulent viscosity does not depend on first or higher derivatives of solution functions. Since turbulent viscosity (2) depends on first derivatives of solution components, type of equations may be undefined. It is feared that the false oscillations generation is resulted from this type

violation at large values of turbulent viscosity. To eliminate this violation, the averaging two steps procedure is used. This procedure provides “smoothing” of turbulent viscosity, consequently, improves convergence to steady state solutions and prevents false unsteadiness.

$$\mu_1 = \int_{-m\Delta\xi}^{m\Delta\xi} \mu(\xi + c, \eta)\,\Omega(m\Delta\xi, c)\,dc, \qquad (4)$$

$$\mu_{fin} = \int_{-m\Delta\eta}^{m\Delta\eta} \mu_1(\xi, \eta + c)\,\Omega(m\Delta\eta, c)\,dc,$$

$$\Omega(\varepsilon, c) = (1.2 - c^2/\varepsilon^2) \Big/ \int_{-\varepsilon}^{\varepsilon} (1.2 - c^2/\varepsilon^2)\,dc.$$

Grids 515×586 and 715×816 are used in calculations. Weight function constant (3) is chosen as C_0=12. Adaptive turbulent viscosity (2) constants are chosen as C_1 =2.5, C_2=0.21 (this value is standard in LES investigations). Parameter m in averaging formulas (4) is equal to 5 for the 515×586 grid and *m*=7 for the 715×816 grid. CFL numbers were limited by 0.5 in previous calculations [6-7] to provide stability of explicit Godunov method. Necessity of more strong limitation is discovered here due to increased values of the Smagirinsky turbulent viscosity near contact discontinuities. So the interval 0.25-0.35 of CFL numbers is kept for Godunov method in present computations. Runge-Kutta method computations are provided with double time steps. As a result this method turns out to be more effective, then Godunov method, despite the fact that Runge-Kutta method requires more operations for one time step.

3. Results and discussion

CFD studies [6,7] shown, that self-oscillations may appear, if two shock waves, induced by braking of free stream by the cylinder and by the tube end, have intersection point closed to the tube edge (signed by *C* in fig.1). Two types of hypersonic self-oscillatory flows are observed in [7].

If the contact discontinuity, issued from this point of intersection, is directed always above the tube edge and moves outside a tube, nearly sinusoidal oscillations of a moderate intensity are observed.

If this contact discontinuity is directed inside or outside the tube alternately, flow contains short time peaks of pressure and density near the tube edge. Such complicated oscillations are classified in [7] as oscillations of the second type.

Present paper is devoted to a search for these two self-oscillatory regimes at free stream Mach numbers of 3.5 to 4.5.

Fig. 2 shows density histories at the point *C* (see fig. 1) for the self-oscillatory flow with free stream Mach number M_∞=4.5. Godunov type method data are marked as *G. m.*, Runge-Kutta method data are marked as *R.-K. m*. This flow is defined by geometry parameters L_{cyl}=1.7 (the cylinder length), R_{cyl} =.3 (the cylinder radius), L_{tub}=1.0 (the channel length), $R_{\min} = R_{tub}$-*h*=1-*h*=.93 (the least channel radius), *h* =.08, *a*=*x*(C)+ 0.25L_{tub}, *b*=*a*+0.1 (see fig. 1 and formulae 1). Density histories, presented in fig. 2, illustrates that this flow is nearly periodic. Calculations for Runge-Kutta method data result the *T*=1.84 period, calculations for Godunov method data result the *T*=1.92 period. Time instant $t=t_0 \approx 12.85$, marked in this fig., corresponds approximately to the minimal value of pressure at the tube edge.

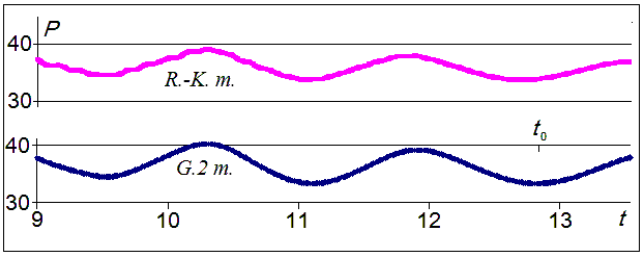

Fig. 2. *Pressure histories*, M_∞ =4.5.

Figs. 3 and 4 show density distributions for the time instants $t=t_0 \approx 12.85$ and for the end time instant $t=t_{end} \approx 13.45$. Godunov type method data for the 515×586 mesh are pictured. Fig. 3 corresponds to

nearly minimal distance of intersection point from the tube edge, fig. 4 corresponds to nearly maximal distance of this point from the tube edge.

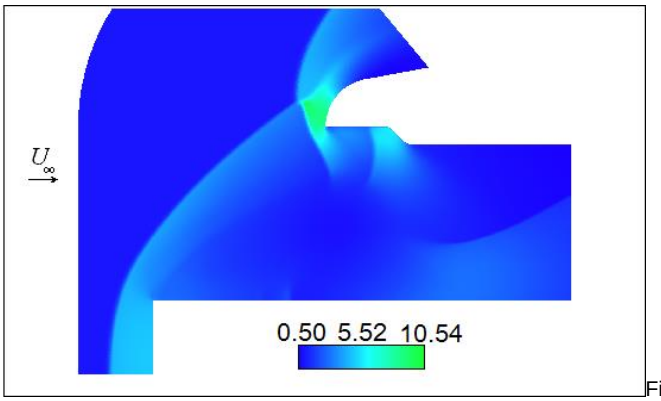

Fig. 3. *The density distribution*, M_∞=4.5, $t=t_0$.

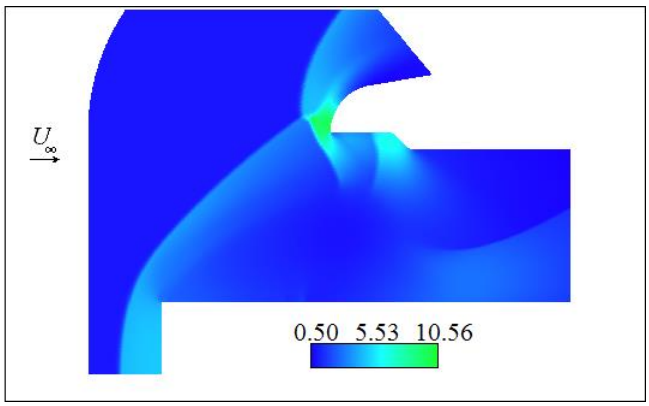

Fig. 4. *The density distribution*, M_∞=4.5, $t=t_{end}$.

It is seen, that the intersection point of two shock waves is placed higher of the tube edge in figs 3-4. So, figs. 2-4 demonstrate first type of oscillations.

Density histories at the tube edge are shown in fig. 5 for free stream Mach number M_∞=4.0. Geometry parameters are L_{cyl}=1.4 (the cylinder length), R_{cyl}=.3 (the cylinder radius), L_{tub}=0.8 (the channel length), $R_{\min}$ = R_{tub} -h=1-h=.96 (the least channel radius), h =.04, a=x(C)+ 0.25L_{tub}, b=a+0.1 (see fig. 1). Pressure histories, presented in fig. 5, illustrates that this flow is nearly periodic. Calculations for Runge-Kutta method data result the T=2.05 period, calculations for Godunov method data result the T=2.02 period. Time instant $t=t_0$≈12.85, marked in this fig., corresponds to a low value of pressure at the tube edge.

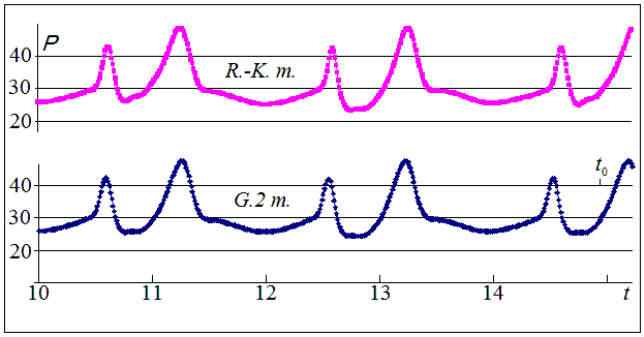

Fig. 5. *Pressure histories*, M_∞ =4.

Figs. 6 and 7 show density distributions for time instants $t=t_0$ and for the end time instant $t=t_{end}$≈15.22. These distributions are pictured for Godunov type method data, received for the grid 515×586 mesh.

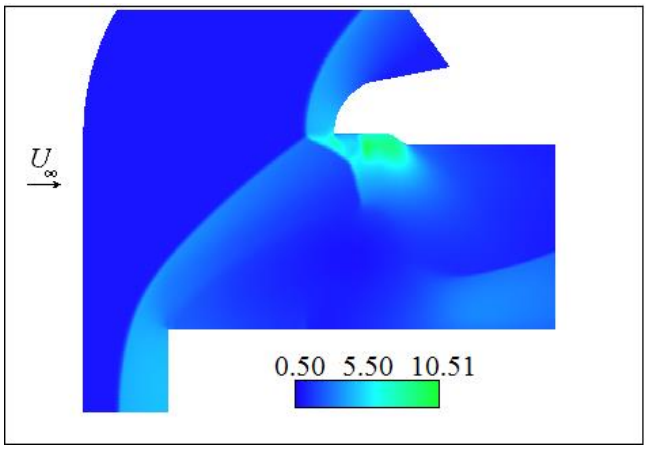

Fig. 6. *The density distribution*, M_∞ =4, $t=t_0$.

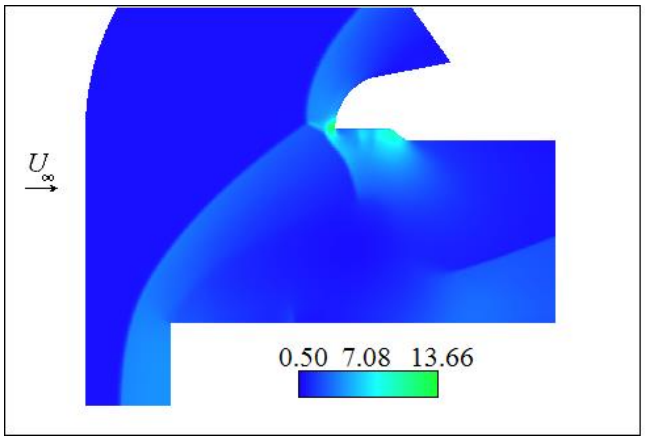

Fig. 7. *The density distribution*, M_∞ =4, $t=t_{end}$.

If to compare figs. 6 and 7, it is seen that the shock waves intersection point in fig. 7 is higher, then this point in fig. 6. Contact discontinuity, issuing from the point of

intersection, changed it's drift direction and began to move above the tube edge, consequently, the current adjoined to the contact discontinuity undergoes sudden braking, which results compression, producing the pressure peak, visible in fig. 5 at the end time instant. These flow oscillations may be classified as oscillations of the second type. Flow regimes of first type are not found for the free stream Mach number M_∞ =4.

The least Mach number for which self-oscillatory flows are found here is 3.5. Fig. 8 shows density histories at point *C* for the flow with M_∞ =3.5. This flow is defined by geometry parameters L_{cyl} =1.8 (the cylinder length), R_{cyl} =.3 (the cylinder radius), L_{tub} =1.3 (the channel length), $R_{\min} = R_{tub} - h = 1 - h = .94$ (the least channel radius), h =.06, $a = x(C) + 0.2L_{tub}$, $b = a + 0.1$ (see fig. 1). Data, shown in fig. 8, are received for the 715 × 816 grid mesh. Initial flow fields for these this calculations are received by linear interpolation from the 515×586 mesh at initial time instant t=7. It is seen, that these density histories are nearly periodic. Calculations for Runge-Kutta method data result the T=2.24 period, calculations for Godunov method data result the T=2.27 period. Time instants $t=t_0 \approx 12.05$ and $t=t_1 \approx 12.55$, marked in fig. 8, correspond approximately to the minimal and maximal values of density.

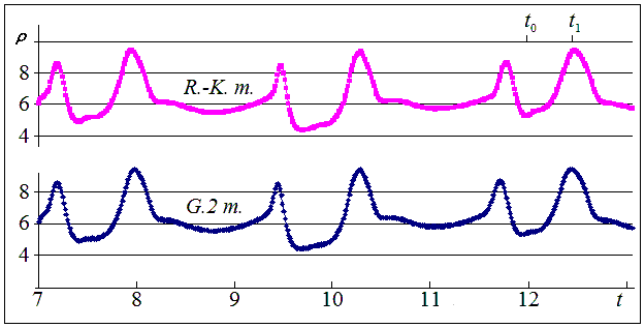

Fig. 8. *Density histories*, M_∞ =3.5.

Density distributions for this flow at time instants $t=t_0$ and $t=t_1$ are shown in figs. 9 and 10. These pictures are received for Runge-Kutta method data.

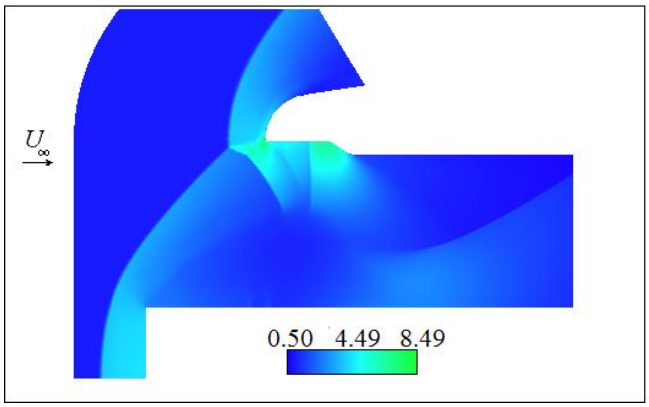

Fig. 9. *Density distributions,* M_∞ =3.5, $t=t_0$.

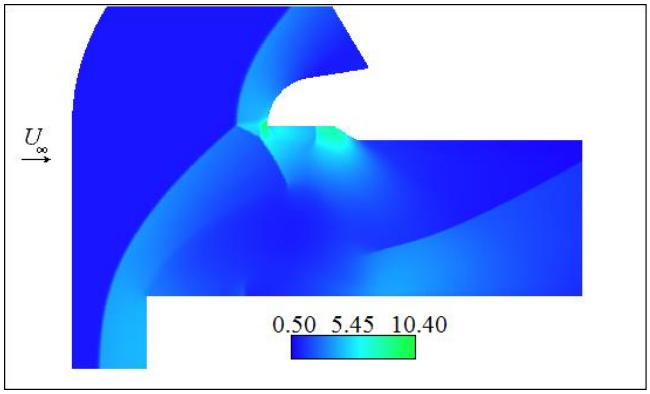

Fig. 10. *Density distributions,* M_∞ =3.5, $t= t_1$.

These two figs. show that the shock waves intersection point in fig. 10 is higher, then this point in fig. 9. Contact discontinuity, issuing from the point of intersection, changed it's drift direction and began to move above the tube edge, consequently, the current adjoined to the contact discontinuity undergoes sudden braking, which results compression, visible in fig. 8 at time instant $t= t_1$. Such flow oscillations may be classified as oscillations of second type.

It seems, that flows of the first type of this family have the oscillation mechanism, similar to this mechanism of flows around spiked bodies [1,8-10]. Namely, a cylinder plays role of a spike, and self-oscillations take place, when the shock wave, induced by braking of free stream near cylinder, and the shock wave, induced by braking of free stream near the tube end, intersect in the vicinity of the tube edge. Similarly, self-oscillations take place near spiked bodies, when the shock wave, induced by a spike, and the shock wave, induced by main body, intersect in the vicinity of main body.

4. Conclusions

Self-oscillatory supersonic flows near the pair cylinder - open channels are found in [6]. Self-oscillatory flows with hypersonic free stream velocities are studied in [7]. Two types of self-oscillatory hypersonic flows are observed in [7]. Self-oscillatory flow of first type takes place, if contact discontinuity, issued from the intersection point, is directed always above the tube edge. Self-oscillatory flows of second type takes place, if contact discontinuity, issued from the intersection point, is directed alternatively above or below the tube edge.

Here these investigations are continued for free stream Mach numbers $3.5 \le M_\infty \le 4.5$. Self-oscillatory flow of the first type is found here only for free stream Mach number $M_\infty = 4.5$. Self-oscillatory flows of the second type are observed for all considered here free stream Mach numbers $M_\infty = 3.5, 4.0, 4.5$.

Neither hypersonic, nor supersonic self-oscillatory regimes are not found, if the interval of cross-sectional area decreasing is absent.

References

[1] V.I. Pinchukov, “Numerical modeling of non-stationary flows with transient regimes”, Comput. Mathem. and Mathem. Phisics, 49(10), 2009, pp. 1844–1852.

[2] V.I. Pinchukov, “Modeling of self-oscillations and a search for new self-oscillatory flows”, Mathematical Models and Computer Simulations, 4(2), 2012, pp. 170–178.

[3] V.I. Pinchukov, “Self-oscillatory flows near blunted bodies, giving off opposite jets: CFD study”, Intern. J. of Engineering and Innovative Technology, 6(5), 2016, pp. 41-46.

[4] V.I. Pinchukov, “Sonic underexpanded jet impinging on the pair open tube – inner cylinder”, Intern. J. of Modern Trends in Engineering and Research, 4(11), 2017, pp. 8-14.

[5] V.I. Pinchukov, “Godunov type methods calculations of unsteady flows near blunted cylinders, giving off opposite jets”, J. of Multidisciplinary Engineering Science Studies (JMESS), 5(10), 2019, pp. 2841-2846.

[6] V.I. Pinchukov, “Self-oscillatory interactions of supersonic streams with cylinders, placed in open channels”, Arxiv.org/papers/1804/1804.08997.pdf, 5 pp.

[7] V. I. Pinchukov. CFD studies of hypersonic self-oscillatory flows near cylinder, placed in open channel with transient cross-sectional area. Journal of Multidisciplinary Engineering Science Studies, V. 6, Issue 9, 2020, 3521-3528.

[8] M. Gauer, A. Paull, “Numerical investigation of a spiked nose cone at supersonic speeds”, J. of Spacecraft and Rockets, 45(3), 2008, pp. 459-471.

[9] D. Sahoo, S. Das, P. Kumar and J. Prasad, “Effect of spike on steady and unsteady flow over a blunt body at supersonic speed”, Acta Astronautica, 128, 2016, pp. 521-533.

[10] R.C. Mehta, “Pressure oscillations over a spiked blunt body at hypersonic Mach number”, Computational Fluid Dynamics J., 9(2), 2008, pp. 88-95.

[11] S.K. Godunov, “A difference method for numerical calculation of discontinuous solutions of the equations of hydrodynamics”, Mat. Sb. (N.S.), 47(89):3, 1959, pp. 271–306.

[12] V.I. Pinchukov, “Numerical solution of the equations of viscous gas by an implicit third order Runge-Kutta scheme”, Comput. Mathem. and Mathem. Physics, 42(6), 2002, pp. 898-907.

[13] P. Woodward, “The numerical simulation of two-dimensional fluid flow with strong shocks”, Journal of Comput. Physics, 54, 1984, pp. 115-173.

[14] J. Smagorinsky, “General circulation experiments with the primitive equations. I. The basic experiment”, Monthly Weather Review, 91, 1963, pp. 99-164.